

Resonant Production of Color Octet Muons at the Future Circular Collider Based Muon-Proton Colliders

Y. C. Acar

*Department of Electrical and Electronics Engineering,
TOBB University of Economics and Technology, Ankara, Turkey**

U. Kaya

*Department of Material Science and Nanotechnology,
TOBB University of Economics and Technology, Ankara, Turkey and
Department of Physics, Faculty of Sciences, Ankara University, Ankara, Turkey[†]*

B. B. Oner

*Department of Material Science and Nanotechnology,
TOBB University of Economics and Technology, Ankara, Turkey[‡]*

We investigate the resonant production of color octet muons in order to explore the discovery potential of the FCC-based μp colliders. It is shown that search potential of μp colliders essentially surpass potential of the LHC and would exceed that of FCC pp collider.

* ycacar@etu.edu.tr

† ukaya@etu.edu.tr

‡ b.oner@etu.edu.tr

I. INTRODUCTION

High energy physics experiments performed in the recent decades show that Standard Model (SM) is consistent in low energy regime. However there are still phenomenological and theoretical problems and questions to be answered. Experimental researches for the new physics, searching these answers on higher energies, rely on recently developing accelerator technologies. Energy frontier lepton colliders seem to be prominent candidates to investigate validity of SM at high energies and they have potentials to reveal novelties that lie beyond the Standard Model (BSM). Producing and colliding muon beams with intense bunches to achieve sufficiently high luminosities is still a promising topic. In this regard, a recent paper of the Muon Accelerator Program (MAP) addressed designs of various center of mass (CM) energy muon colliders (μC) from 126 GeV (Higgs-factory) to multi-TeV (energy frontier) options [1]. Also ultimate case muon colliders with CM energy up to 100 TeV was considered in another study and parameters of these colliders are given [2].

Developing technology of lepton colliders make high luminosity and high CM energy lepton-hadron colliders possible. In this manner, one can utilize advantages of their vital role in understanding the fundamental structure of the matter using highest energy hadron beams which will be provided by the Future Circular Collider (FCC) [3]. In the near future, it is expected that construction of μp machines can also be considered depending on solutions of the principal issues of the $\mu^+\mu^-$ colliders.

Muon-proton colliders were proposed two decades ago. Construction of additional proton ring in $\sqrt{s} = 4$ TeV muon collider tunnel was suggested in [4] to handle μp collider with the same CM energy. However, luminosity value, namely $L_{\mu p} = 3 \times 10^{35} \text{ cm}^{-2} \text{ s}^{-1}$, was extremely over estimated, realistic value for this option should be three orders smaller [5]. Then, construction of additional 200 GeV energy muon ring in the Tevatron tunnel in order to handle $\sqrt{s} = 0.9$ TeV μp collider with $L_{\mu p} = 10^{32} \text{ cm}^{-2} \text{ s}^{-1}$ was considered in [6]. Also in Ref. [5] the ultimate case of muon beam with 50 TeV energy [2] had been thought as an option for 100 TeV CM energy μp colliders assuming that 50 TeV proton ring would be added into the μC tunnel and a luminosity value $\sim 10^{33} \text{ cm}^{-2} \text{ s}^{-1}$ is estimated. FCC based muon-proton and muon-lead ion colliders' main parameter calculations are performed in a recent paper which considers beam-beam effects and a basic collider parameter optimization [7].

In Ref. [8], physics potentials of μp colliders with several energy and luminosity options (from $\sqrt{s} = 314$ GeV, $L_{\mu p} = 0.1 \text{ fb}^{-1}$ per year to $\sqrt{s} = 4899$ GeV, $L_{\mu p} = 280 \text{ fb}^{-1}$ per year) were studied. Sensitivity reach of each collider were calculated for some BSM phenomena such as R-parity violating squarks, leptoquarks, leptogluons and extra-dimensions. Similarly, R-parity violating resonances were examined for Tevatron based μp collider with $\sqrt{s} = 0.9$ TeV and $L_{\mu p} = 10^{32} \text{ cm}^{-2} \text{ s}^{-1}$ in [9]. In a recent study excited muon production is analyzed at muon-hadron colliders based on the FCC [10].

This paper shows a follow up work of our previous study which was based on the search potential of the FCC-based ep colliders on color octet electrons [11] (besides, there are number of papers devoted to the study of color octet electron production at the LHC [12–15] and LHeC [16–18]).

We now consider another design, namely, construction of muon ring tangential to the FCC which is schematically shown in Fig. 1. The aim is to achieve highest possible CM energies in lepton-hadron colliders in order to make some of the BSM physics process researches possible. Here, physics potential of these future colliders are revealed quantitatively exploring resonant production of color octet muons. Parameters of the FCC-based muon proton colliders are given in Table I. The first four colliders [7] use the most recent design parameters of MAP [1]. The last row corresponds to the ultimate case with 20 TeV muon beam in the FCC tunnel. 20 TeV choice is due to synchrotron radiation loss of muons which is desired to be limited at 1 GeV/turn for a muon accelerator with 100 km circumference [19].

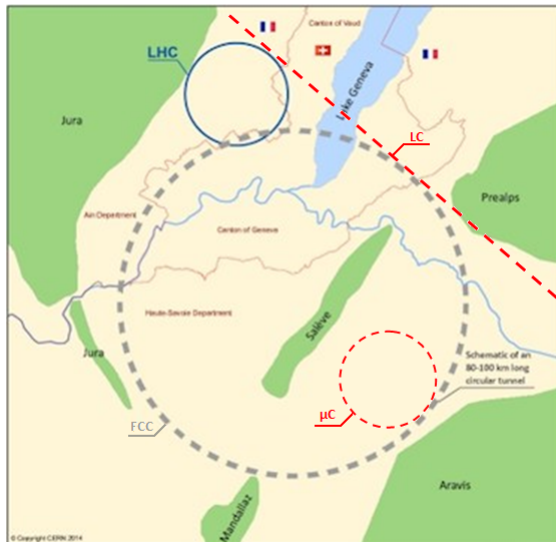


Figure 1. Possible configuration of FCC, linear collider (LC) and muon collider (μ C).

Table I. Main parameters of the FCC based μp colliders.

Collider Name	E_μ , TeV	CM Energy, TeV	L_{int} , fb^{-1} per year
$\mu 63 \otimes \text{FCC}$	0.063	3.55	0.02
$\mu 750 \otimes \text{FCC}$	0.75	12.2	5
$\mu 1500 \otimes \text{FCC}$	1.5	17.3	5
$\mu 3000 \otimes \text{FCC}$	3.0	24.5	5
$\mu 20000 \otimes \text{FCC}$	20	63.2	10

The rest of the paper is organized as follows. In Section II, we present phenomenology of color octet muon. Section III covers signal-background analyses and closes by giving the results of discovery limit searches of muon-proton colliders. Section IV addresses the determination of compositeness scales via muon-proton collider options under two possibilities regarding results of the FCC. Finally, Section V contains summary of the obtained results.

II. COLOR OCTET MUON

One of the possible answer to the problems mentioned in the Introduction may hide behind the concept of compositeness. Fermion-scalar and three-fermion models are the most proper options which enable known SM leptons to be constructed from more fundamental particles, namely preons. If SM leptons are composed of color triplet fermions and color triplet scalars, then both fermion-scalar and three-fermion models predict at least one color octet partner to the color singlet leptons:

$$\ell = (F\bar{S}) = 3 \otimes \bar{3} = 1 \oplus 8, \quad (1)$$

$$\ell = (FFF) = 3 \otimes 3 \otimes 3 = 1 \oplus 8 \oplus 8 \oplus 10. \quad (2)$$

Interaction lagrangian of ℓ_8 with leptons and gluons can be written as

$$L = \frac{1}{2\Lambda} \sum_l \{ \bar{\ell}_8^\alpha g_s G_{\mu\nu}^\alpha \sigma^{\mu\nu} (\eta_L \ell_L + \eta_R \ell_R) + h.c. \}, \quad (3)$$

where g_s is strong coupling constant, Λ denotes compositeness scale, $G_{\mu\nu}$ is gluon field strength tensor, $\ell_{L(R)}$ stands for left (right) spinor components of lepton, $\ell = e, \mu, \tau$; $\sigma^{\mu\nu}$ is the antisymmetric tensor ($\sigma^{\mu\nu} = \frac{i}{2} [\gamma^\mu, \gamma^\nu]$), $\eta_L(\eta_R)$ symbolizes chirality factor. Keeping in mind leptonic chiral invariance ($\eta_L\eta_R = 0$), we take $\eta_L = 1$ and $\eta_R = 0$. Decay width of ℓ_8 given by

$$\Gamma(\ell_8 \rightarrow \ell + g) = \frac{\alpha_s M_{\ell_8}^3}{4\Lambda^2}, \quad (4)$$

where $\alpha_s = g_s/4\pi$. Dependence of the decay width on the mass of μ_8 is presented in Fig. 2 for $\Lambda = M_{\mu_8}$ and $\Lambda = 100$ TeV cases.

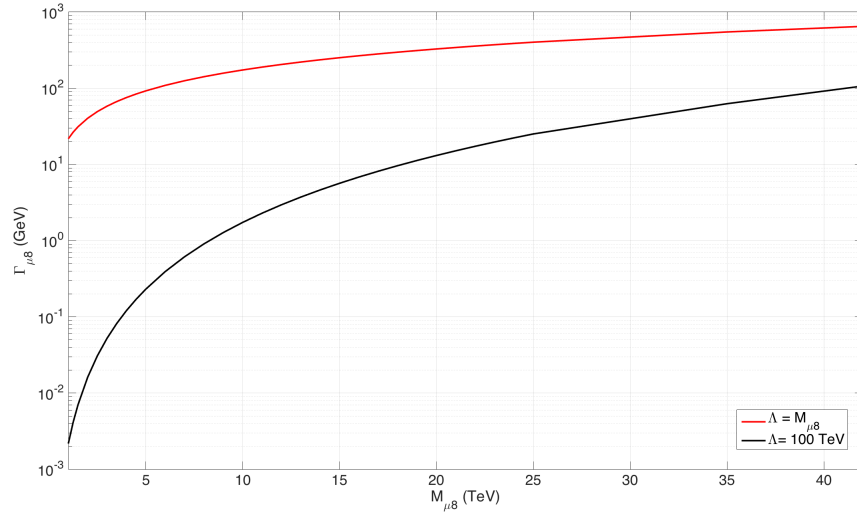


Figure 2. Color octet muon decay width for $\Lambda = M_{\mu_8}$ and $\Lambda = 100$ TeV.

The resonant μ_8 production (see Figure 3) cross sections for different stages of the FCC based μp colliders from Table I are calculated using MadGraph5 event generator [20]. CTEQ6L1 parametrization [21] is used as parton distribution function and results are presented in Figure 4. MadGraph5-Pythia6 interface was used for parton showering and hadronization [22].

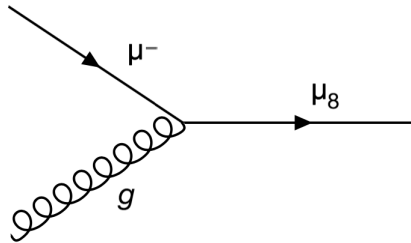


Figure 3. Feynman diagram for the resonant μ_8 production.

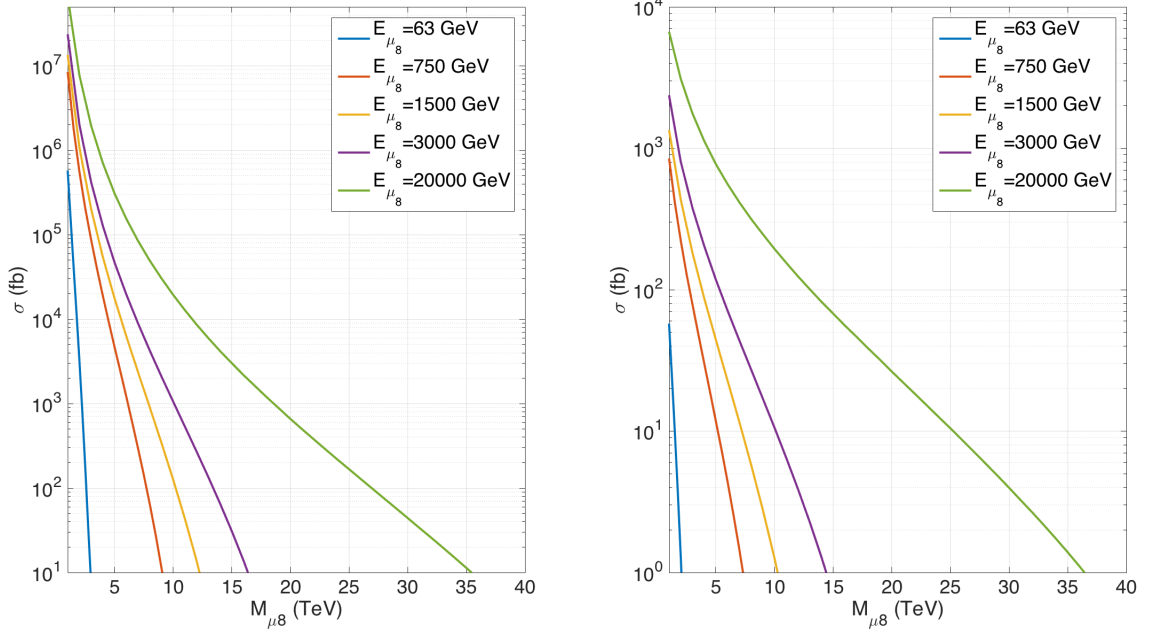


Figure 4. Resonant color octet muon production at the FCC based μp colliders given in Table I for (a) $\Lambda = M_{\mu_8}$ and for (b) $\Lambda = 100$ TeV.

III. SIGNAL - BACKGROUND ANALYSIS

In this section, results of the numerical calculations are shown for the process $p\mu \rightarrow j\mu$ to analyze the search potential of the FCC based muon-proton colliders on the μ_8 discovery via resonant production within $\Lambda = M_{\mu_8}$ scenario. MadGraph5 [20] with CTEQ6L1 [21] parton distribution function was used as event generator and MadGraph5-Pythia6 [22] interface was used for parton showering and hadronization for the calculation of the signal and background processes.

A staged approach is applied to determine mass limits as follows. $\mu 63 \otimes \text{FCC}$, the μp collider with minimum CM energy, is chosen as the initial collider which discovery limit of μ_8 mass is to be sought. After discovery limit is determined, a worse scenario is considered where μ_8 is assumed to have a larger mass. A higher CM energy μp collider assumes that the previous collider had excluded μ_8 mass up to the corresponding discovery limit and applies necessary cuts regarding this assumption. Latter colliders follow the rows of Table I respectively. This procedure ends with the ultimate μp collider with CM energy 63.2 TeV given as the last row of the Table I.

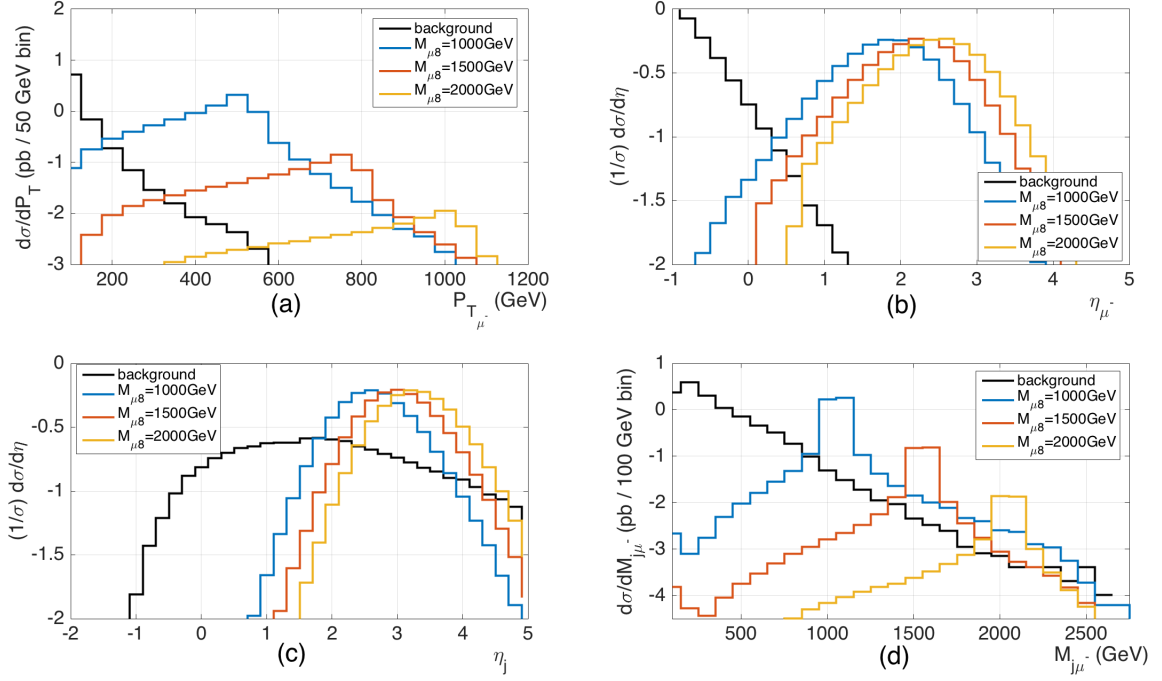


Figure 5. a) Transverse momentum distributions of final state jets (and muons), b) pseudorapidity distributions of final state muons, c) pseudorapidity distributions of final state jets and d) invariant mass distributions for signal and background at $\mu 63 \otimes \text{FCC}$ after generic cuts.

Kinematical distributions of $\mu 63 \otimes \text{FCC}$ with generic cuts ($p_{T_\mu} > 20$ GeV, $p_{T_j} > 30$ GeV) are given in Fig. 5. Reconsideration of the ATLAS/CMS results on the search for the second generation leptoquarks [23, 24] (which has same decay channel as μ_8) leads us to the strongest current limit on the color octet muon mass, $M_{\mu_8} \gtrsim 1$ TeV. Therefore we chose discovery cut for transverse momentum as $p_T > 350$ GeV on our initial μp collider. In order to suppress the background while keeping the signal cross section as much as possible, following pseudorapidity cuts are applied: $2.00 < \eta_j < 4.00$, $0.5 < \eta_\mu < 4.74$. Maximum possible value of η_μ and η_j is taken 4.74 which corresponds to 1° in proton direction. This value can be covered by very forward detector as in the LHeC case [25]. Effects of these cuts can be seen from Fig. 6 where invariant mass of μ_8 is reconstructed from final state particles μ and leading-jet after applying discovery cuts.

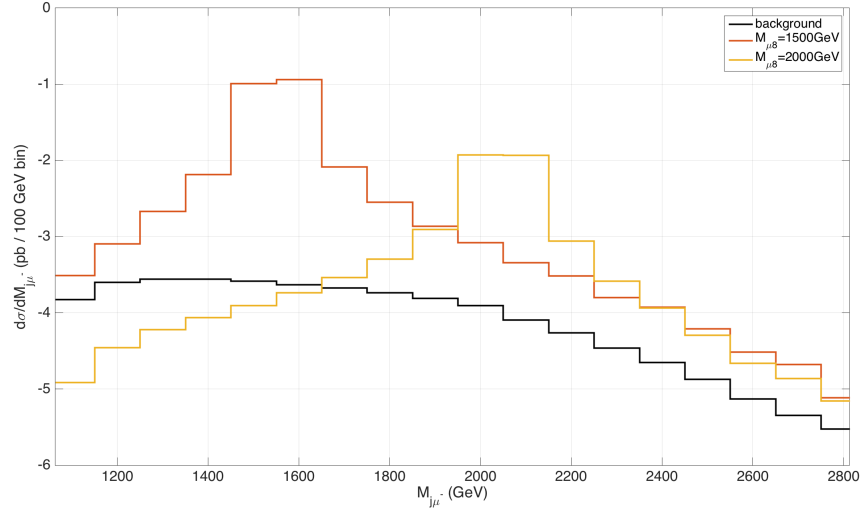


Figure 6. Invariant mass distributions for signal and background at $\mu 63 \otimes \text{FCC}$ after discovery cuts.

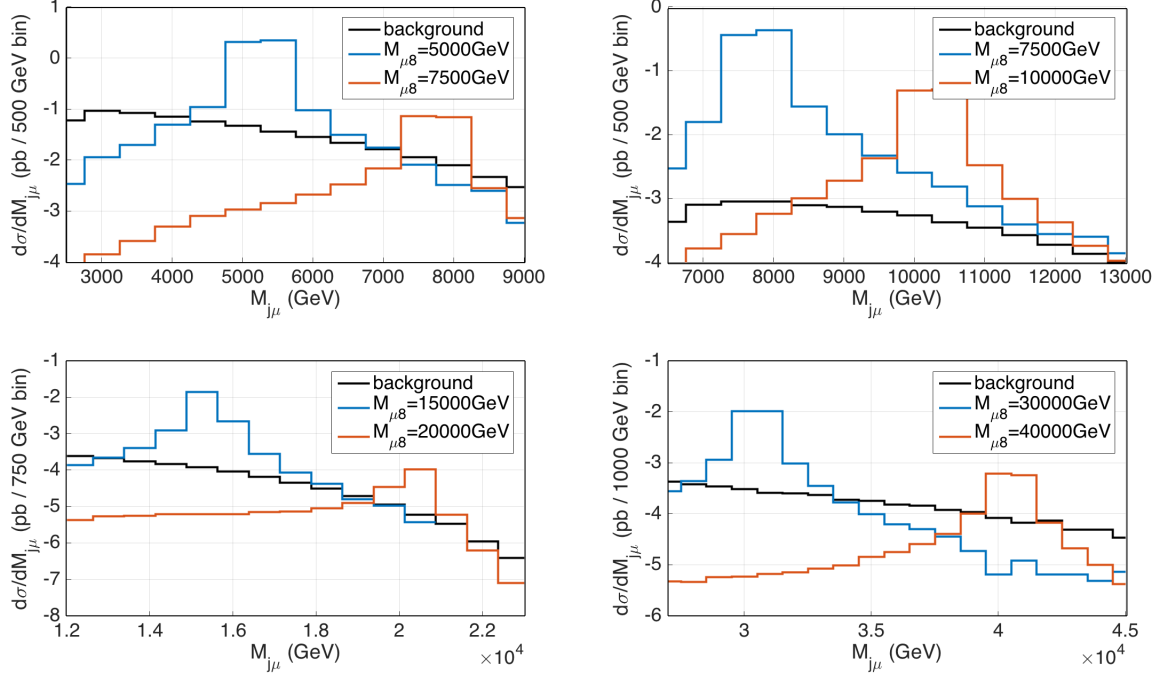
Statistical significance (SS) is calculated using the formula below:

$$SS = \sqrt{2 L_{int}} \sqrt{(\sigma_S + \sigma_B) \ln(1 + (\sigma_S / \sigma_B)) - \sigma_S} \quad (5)$$

where σ_S and σ_B denote cross-section values of signal and background, respectively. Integrated luminosity values, L_{int} , of each collider per year is estimated in [7]. Discovery ($SS = 5$) and observation ($SS = 3$) limits for 0.02 fb^{-1} $\mu 63 \otimes \text{FCC}$ integrated luminosity are found to be 2380 and 2460 GeV, respectively. Regarding these results of the minimum energy μp collider, $p_T > 800$ GeV is considered appropriate for the next stage $\mu 750 \otimes \text{FCC}$ and similar analyses are performed. These consecutive calculations give us mass reach of each collider as given in Table II. Applied discovery cuts are also given in the same table and mass window formulation is kept same for all calculations: $M_{\mu 8} - 2\Gamma_{\mu 8} < M_{\mu 8} < M_{\mu 8} + 2\Gamma_{\mu 8}$. Invariant mass distributions after discovery cuts related to higher energy colliders are presented in Fig. 7.

Table II. Kinematical discovery cuts and observation (3σ) and discovery (5σ) limits for μ_8 at different μp colliders.

Collider Name	L_{int}, fb^{-1}	Kinematical Cuts					M_{μ_8}, TeV	
		$p_{T_{min}} \text{ (GeV)}$	$\eta_{\mu_{min}}$	$\eta_{\mu_{max}}$	$\eta_{j_{min}}$	$\eta_{j_{max}}$	3σ	5σ
$\mu 63 \otimes \text{FCC}$	0.02	350	0.5	4.74	2.0	4.0	2.46	2.38
$\mu 750 \otimes \text{FCC}$	5	800	-1.3	4.74	1.0	4.1	9.60	9.21
$\mu 1500 \otimes \text{FCC}$	5	3000	-1.7	4.74	0.7	3.9	13.8	13.2
$\mu 3000 \otimes \text{FCC}$	5	4400	-2.1	4.74	0.3	3.5	18.9	18.1
$\mu 20000 \otimes \text{FCC}$	10	6000	-2.7	4.74	-0.7	2.7	42.7	41.5

Figure 7. Invariant mass distributions for signal and background at a) $\mu 750 \otimes \text{FCC}$, b) $\mu 1500 \otimes \text{FCC}$, c) $\mu 3000 \otimes \text{FCC}$ and for d) the ultimate case $\mu 20000 \otimes \text{FCC}$ colliders after discovery cuts.

IV. LIMITS ON COMPOSITENESS SCALE

If the μ_8 is discovered by FCC-pp option, μp colliders will give opportunity to estimate compositeness scale. In this regard, two distinct possibilities should be considered:

- a) μ_8 is discovered by FCC but not observed at μ -FCC. In this case one can put lower limit on compositeness scale,
- b) μ_8 is discovered by FCC and also observed at μ -FCC. In this case one can determine compositeness scale.

In this section we present the analysis of these two possibilities for four different benchmark points, namely, $M_{\mu_8} = 2.5, 5, 7.5$ and 10 TeV.

A. μ_8 is discovered by FCC but not observed at μ -FCC

If we assume that μ_8 mass is found out by FCC results then it is possible to determine optimal cuts for given M_{μ_8} at the μ -FCC colliders. Let us start by consideration of $M_{\mu_8} = 5.0$ TeV at $\mu 750 \otimes \text{FCC}$.

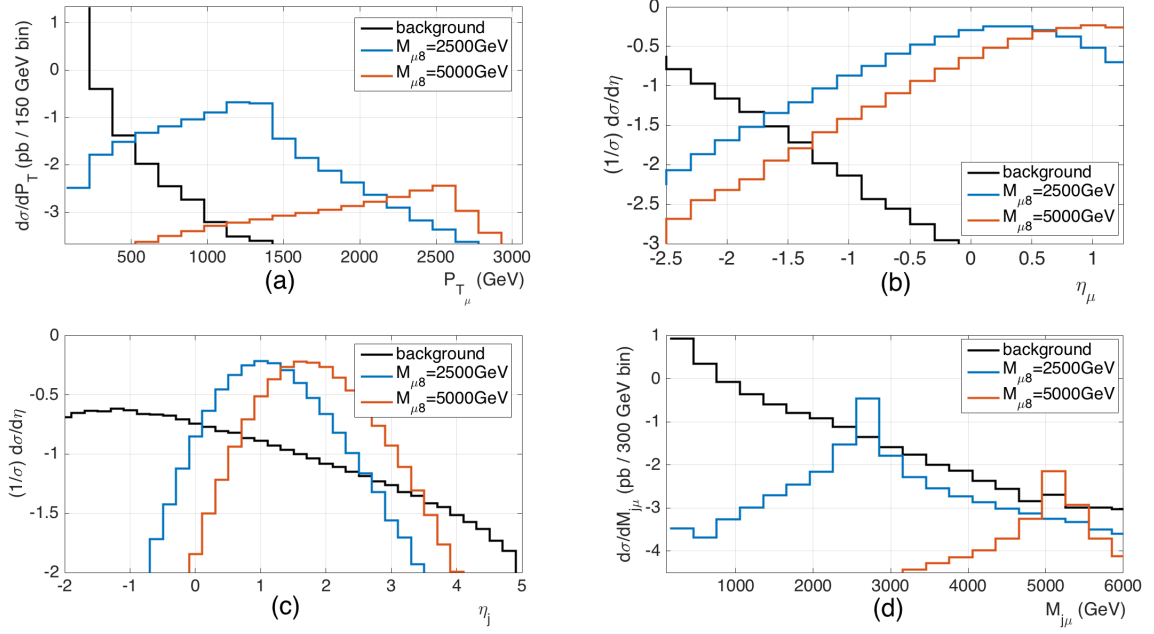


Figure 8. a) Transverse momentum distributions of final state jets (and muons), b) pseudorapidity distributions of final state muons, c) pseudorapidity distributions of final state jets and d) invariant mass distributions for signal and background at $\mu 750 \otimes \text{FCC}$ after generic cuts.

It is seen from Fig. 8 that $-1.3 < \eta_\mu < 4.74$ and $0.7 < \eta_j < 3.3$ cuts drastically decrease the background whereas the signal is slightly affected. Similar cuts are determined for other μ -FCC collider options and $M_{\mu 8}$ values and these optimal cuts are presented in Table III. Invariant mass window $0.99M_{\mu 8} < M_{\mu j} < 1.01M_{\mu 8}$ has been used in this particular analysis. $\mu 63 \otimes \text{FCC}$ collider is not included in this section due to its remarkably low potential compared to the other options.

Table III. Optimal cuts for determination of compositeness scale lower bounds.

Collider	Cut Type	$M_{\mu 8} = 2.5 \text{ TeV}$		$M_{\mu 8} = 5.0 \text{ TeV}$		$M_{\mu 8} = 7.5 \text{ TeV}$		$M_{\mu 8} = 10 \text{ TeV}$	
		min	max	min	max	min	max	min	max
$\mu 750 \otimes \text{FCC}$	η_μ	-1.7	4.74	-1.3	4.74	-1.2	4.74	-	-
	η_j	0.2	2.6	0.7	3.3	1.0	3.9	-	-
	Mass Window (GeV)	2475	2525	4950	5050	7425	7575	-	-
$\mu 1500 \otimes \text{FCC}$	η_μ	-2.3	4.74	-2.0	4.74	-1.8	4.74	-1.7	4.74
	η_j	-0.6	1.9	-0.1	2.7	0.4	3.1	0.5	3.5
	Mass Window (GeV)	2475	2525	4950	5050	7425	7575	9900	10100
$\mu 3000 \otimes \text{FCC}$	η_μ	-2.9	4.74	-2.7	4.74	-2.5	4.74	-2.3	4.74
	η_j	-1.4	1.4	-0.8	2.1	-0.4	2.6	-0.2	3.1
	Mass Window (GeV)	2475	2525	4950	5050	7425	7575	9900	10100
$\mu 20000 \otimes \text{FCC}$	η_μ	-3.9	4.74	-3.5	4.74	-3.3	4.74	-3.2	4.74
	η_j	-3.0	-0.9	-2.5	0.1	-2.1	0.5	-1.9	1.0
	Mass Window (GeV)	2475	2525	4950	5050	7425	7575	9900	10100

Applying cuts presented in Table III and $p_T > 350 \text{ GeV}$ for all cases one can estimate achievable lower limits on compositeness scale. Using Eq. 5 we obtain Λ values given in Table IV. As expected, lower bounds on compositeness scale is decreased with increasing value of the μ_8 mass. It is seen that multi-hundred TeV lower bounds can be put on compositeness scale if μ_8 is discovered at the FCC and not observed at any $\mu \otimes \text{FCC}$.

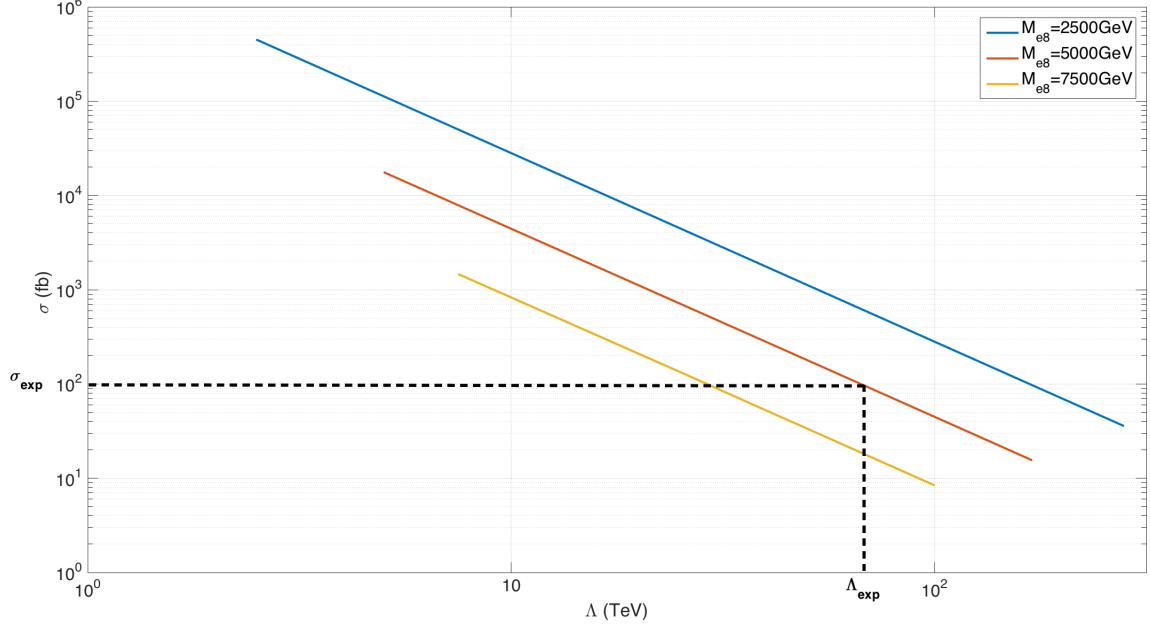


Figure 9. Cross section distributions with respect to compositeness scale for $\mu 1500 \otimes \text{FCC}$ collider

Table IV. Lower limits on compositeness scale in TeV units at the FCC based μp colliders.

Collider	L_{int}, fb^{-1}	$M_{e_8} = 2.5 \text{ TeV}$		$M_{e_8} = 5.0 \text{ TeV}$		$M_{e_8} = 7.5 \text{ TeV}$		$M_{e_8} = 10 \text{ TeV}$	
		3σ	5σ	3σ	5σ	3σ	5σ	3σ	5σ
$\mu 750 \otimes \text{FCC}$	5	270	210	170	130	50	35	-	-
$\mu 1500 \otimes \text{FCC}$	5	360	280	220	170	130	100	55	40
$\mu 3000 \otimes \text{FCC}$	5	475	370	320	245	230	170	140	105
$\mu 20000 \otimes \text{FCC}$	10	1390	1080	850	655	515	400	315	246

B. μ_8 is discovered by FCC and observed at $\mu\text{-FCC}$

In this case, the value of cross section at μp colliders which is inversely proportional to Λ^2 gives opportunity to determine compositeness scale directly. As an example, let us consider $\mu 1500 \otimes \text{FCC}$ case. In Fig. 9 we present Λ dependence of μ_8 production cross section for $M_{\mu_8} = 2.5, 5, 7.5 \text{ TeV}$. Supposing that FCC discovers μ_8 with 5 TeV mass and $\mu 1500\text{-FCC}$ measure cross section as $\sigma_{exp} \sim 100 \text{ fb}$, one can derive compositeness scale as $\Lambda_{exp} \simeq 70 \text{ TeV}$.

V. CONCLUSION

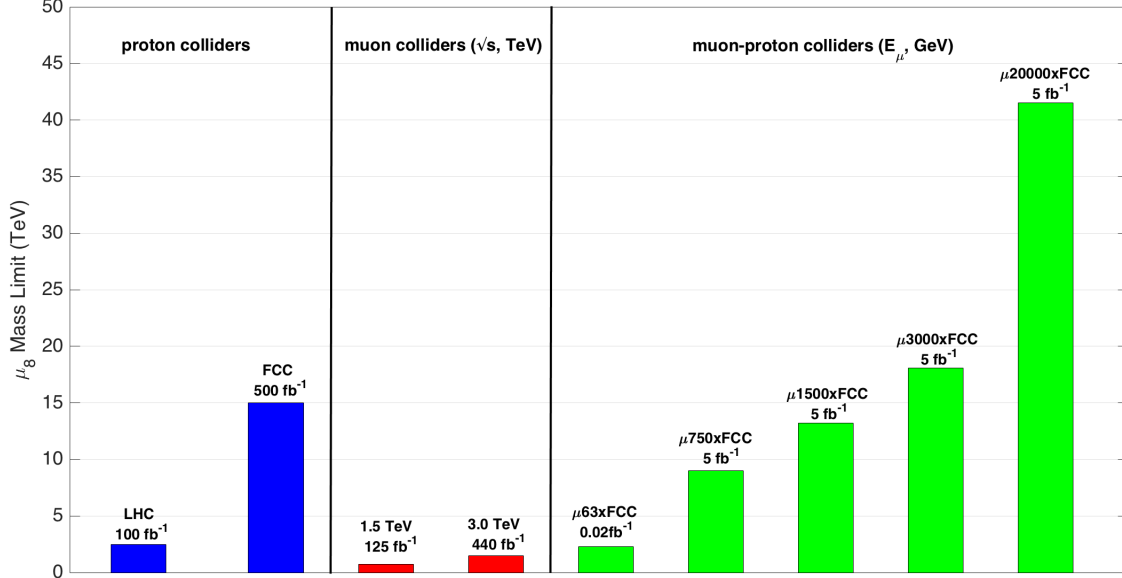


Figure 10. Mass discovery limits ($SS = 5$) of the color octet muon regarding different type of colliders, i.e. proton, muon and muon-proton.

Discovery mass limit for μ_8 at the muon, proton and FCC based μp colliders are shown in Fig. 10. It is obvious that discovery mass limit for pair production of μ_8 at muon colliders are approximately half of CM energies. Discovery mass limit value for LHC and FCC are obtained by rescaling ATLAS/CMS second generation LQ results [23, 24] using the method developed by G. Salam and A. Weiler [26]. As can be seen from the Fig. 10, FCC based μp colliders with discovery limit up to 40 TeV are most advantageous among the other collider options for μ_8 searches. Moreover, FCC based μp colliders will give opportunity to probe compositeness up to PeV scale.

ACKNOWLEDGMENTS

This study is supported by TUBITAK under the grant no 114F337. Authors are grateful to Saleh Sultansoy for useful discussions. Authors are also grateful to Subhadip Mitra and Tanumoy Mandal for sharing leptogluon MadGraph model file.

-
- [1] J.P. Delahaye *et al.*, Enabling intensity and energy frontier science with a muon accelerator facility in the U.S., arXiv:1308.0494v2 [physics.acc-ph].
 - [2] B.J. King, Parameter Sets for 10 TeV and 100 TeV Muon Colliders, and their Study at the HEMC'99 Workshop, arXiv:physics/0005008 [physics.acc-ph].
 - [3] FCC web page: <https://fcc.web.cern.ch>.
 - [4] I.F. Ginzburg, "Physics at future e p, gamma p (linac-ring) and mu p colliders", Turk J. Phys 22, 607 (1998).
 - [5] S. Sultansoy, "The post-HERA era: brief review of future lepton-hadron and photon-hadron colliders", DESY 99-159, arXiv:hep-ph/9911417v2.
 - [6] V.D. Shiltsev, "An asymmetric muon proton collider: luminosity consideration", in Proceedings of 1997 Particle Accelerator Conference, 1998 (Vancouver, British Columbia, Canada), p. 420.
 - [7] Y.C. Acar *et al.*, "FCC Based Lepton-Hadron and Photon-Hadron Colliders: Luminosity and Physics", arXiv:1608.02190 [physics.acc-ph].
 - [8] K. Cheung, "Muon-proton colliders: Leptoquarks, contact interactions and extra dimensions", AIP Conference Proceedings 542 (2000) 160.

- [9] M. Carena, D. Choudhury, C. Quigg, S. Raychaudhuri, "Study of R-parity violation at a $\mu\mu$ collider", Phys. Rev. D 62(9) (2000), arXiv: 095010.
- [10] A. Caliskan, S.O. Kara, A. Ozansoy, "Excited muon searches at the FCC based muon-hadron colliders", arXiv:1701.03426 [hep-ph].
- [11] Y.C. Acar, U. Kaya, B.B. Oner, and S. Sultansoy, "Color octet electron search potential of the FCC based e-p colliders", arXiv:1605.08028v2 [hep-ph].
- [12] A. Celikel, M. Kantar, S. Sultansoy, "A search for sextet quarks and leptogluons at the LHC", Phys. Lett. B. 443(1) (1998).
- [13] T. Mandal and S. Mitra, "Probing color octet electrons at the LHC", Phys. Rev. D., 87(9) (2013), arXiv:1211.6394v2 [hep-ph].
- [14] D. Gonçalves-Netto, D. López-Val, K. Mawatari, I. Wigmore, T. Plehn, "Looking for leptogluons", Phys. Rev. D., 87(9) (2013), arXiv:1303.0845v1 [hep-ph].
- [15] T. Mandal, S. Mitra, S. Seth, "Probing compositeness with the CMS $eejj$ & eej data", Phys. Lett. B. 758 (2016), arXiv:1602.01273v2 [hep-ph].
- [16] A. Celikel and M. Kantar, "Resonance Production of New Resonances at ep and γp Colliders", Tr. J. of Physics 22 (1998) 401.
- [17] M. Sahin, S. Sultansoy and S. Turkoz, "Resonant production of color octet electron at the LHeC", Phys. Lett. B 689 (2010) 172.
- [18] M. Sahin, "Resonant production of spin-3/2 color octet electron at the LHeC", Acta Physica Polonica B 45 (2014) 1811.
- [19] S. Sultansoy talk at 1st FCC Physics Workshop (CERN), <https://indico.cern.ch/event/550509/contributions/2413830>.
- [20] J. Alwall *et al.*, "The automated computation of tree-level and next-to-leading order differential cross sections, and their matching to parton shower simulations", JHEP 2014(7) (2014); arXiv:1405.0301v2 [hep-ph].
- [21] D. Stump *et al.*, "Inclusive jet production, parton distributions and the search for new physics", JHEP 0310 (2003) 046.
- [22] T. Sjostrand, S. Mrenna, and P.Z. Skands, "PYTHIA 6.4 physics and manual," JHEP 0605 (2006) 026, arXiv:hepph/0603175 [hep-ph].
- [23] V. Khachatryan *et al.* (CMS Collaboration), "Search for pair production of first and second generation leptoquarks in proton-proton collisions at $\sqrt{s}=8$ TeV", Phys. Rev. D 93, (2016) 032004.
- [24] ATLAS Collaboration, "Search for scalar leptoquarks in pp collisions at $\sqrt{s}=13$ TeV with the ATLAS experiment", arXiv:1605.06035v2 [hep-ex].
- [25] J.L. Abelleira Fernandez *et al.* (LHeC Study Group), "A Large Hadron Electron Collider at CERN: Report on the Physics and Design Concepts for Machine and Detector", J. Phys. G: Nucl. Part. Phys. 39, (2012) 075001.
- [26] G. Salam and A. Weiler, "The Collider Reach project", <http://collider-reach.web.cern.ch/collider-reach>.